

# RSC Advances



This is an *Accepted Manuscript*, which has been through the Royal Society of Chemistry peer review process and has been accepted for publication.

*Accepted Manuscripts* are published online shortly after acceptance, before technical editing, formatting and proof reading. Using this free service, authors can make their results available to the community, in citable form, before we publish the edited article. This *Accepted Manuscript* will be replaced by the edited, formatted and paginated article as soon as this is available.

You can find more information about *Accepted Manuscripts* in the [Information for Authors](#).

Please note that technical editing may introduce minor changes to the text and/or graphics, which may alter content. The journal's standard [Terms & Conditions](#) and the [Ethical guidelines](#) still apply. In no event shall the Royal Society of Chemistry be held responsible for any errors or omissions in this *Accepted Manuscript* or any consequences arising from the use of any information it contains.

## ARTICLE

# Using poly(3,4-ethylenedioxythiophene) containing a carbamate linker as a platform to develop electrodeposited surfaces with tunable wettability and adhesion

Cite this: DOI: 10.1039/x0xx00000x

Received 00th January 2012,  
Accepted 00th January 2012

DOI: 10.1039/x0xx00000x

[www.rsc.org/](http://www.rsc.org/)

Caroline R. Szczepanski, Thierry Darmanin, and Frederic Guittard\*

To control the wettability of polymer interfaces with water without using perfluorinated chains, the 3,4-ethylenedioxythiophene (EDOT) monomer and its derivatives have been good candidates for surfaces formed by electrodeposition. In this work, a series of original EDOT-based monomers were studied. A carbamate linker was used to introduce alkyl and aromatic substituents onto the EDOT-monomer, and the side groups were found to significantly influence the resulting surface structuration and wettability. As the chain length of alkyl substituent increases, rougher more hydrophobic surfaces form. With significantly long alkyl side groups ( $>C_6$ ), superhydrophobic properties including water contact angles ( $\theta_{water}$ ) up to  $158^\circ$  were observed despite intrinsic hydrophilicity of the polymers. In general the monomers with aromatic substituents formed smoother surfaces. Oleophobicity was tested using diiodomethane, and it was found the wetting state varied with side group: longer alkyl ( $>C_8$ ) and aromatic substituents were completely penetrated by diiodomethane (Wenzel state of wetting), while shorter alkyl substituents followed the Cassie Baxter state. With a relatively facile synthetic route to develop the monomers, these polymers are very attractive for anti-bioadhesion, anti-icing, and anti-fog applications.

## 1. Introduction

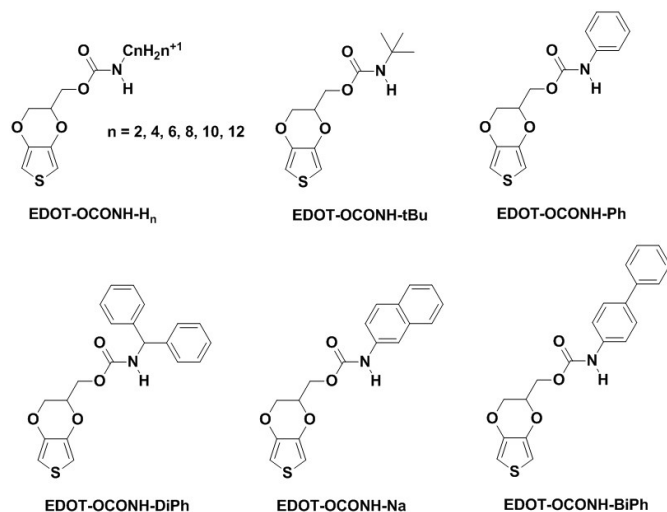
For many applications, surfaces with strong hydrophobicity are necessary. More specifically superhydrophobicity, defined by a contact angle with water ( $\theta_{water}$ )  $> 150^\circ$  and low hysteresis is highly desirable since this unique wetting behavior is attractive for anti-icing,<sup>1-3</sup> anti-fog,<sup>4,5</sup> anti-bioadhesion,<sup>6</sup> and separations applications.<sup>7,8</sup> Through the study and analysis of natural surfaces with superhydrophobic behavior, it has been determined that both surface chemical composition and topography are critical factors in obtaining strongly anti-wetting behavior.<sup>9-13</sup> One can look to the Cassie-Baxter<sup>14</sup> and Wenzel<sup>15</sup> equations of wetting to see the significant influence of surface roughness on the observed contact angle with water ( $\theta_{water}$ ). The adhesive behavior of a surface depends strongly on the intrinsic hydrophobicity or hydrophilicity of the surface as well as the overall wetting state whether it be Cassie-Baxter or Wenzel.<sup>16-21</sup>

To augment and control surface roughness, two types of methods have been identified: top-down and bottom-up.<sup>22</sup> With top-down approaches a bulk surface is carved or etched to generate roughness, one example being the use of plasma treatment. With bottom-up approaches the controlled growth of

new surfaces is used to generate roughness. Examples of bottom-up approaches include layer-by-layer assembly, self-organization, and electro-chemical polymerization. Within these techniques, electro-chemical polymerization has been particularly appealing as it is a cost-effective and easily reproducible method to form surfaces of conductive polymers with controllable morphology.<sup>23</sup> The 3,4-ethylenedioxythiophene (EDOT) monomer and its derivatives have been good candidates for the development of superhydrophobic surfaces by electrodeposition due to its high conductivity and quick polymerization.<sup>24-27</sup> It has been shown that the resulting wettability and morphology of surfaces formed by PEDOT-deposition can be tailored by grafting of a hydrophobic side group. Additionally, recent works have demonstrated that the type of linker used to attach a side-group to EDOT can also influence the interaction of the surface with both oils and water.<sup>27</sup>

In this work, we report the synthesis and electrodeposition of a new series of EDOT-based monomers. A carbamate linker was used to integrate various side groups onto the EDOT-monomer, influencing the structuration of surfaces after electropolymerization. The side groups integrated were *n*-alkyl, *br*-alkyl and aromatic (phenyl, diphenyl, naphthalene, biphenyl)

in nature, and all synthesized monomers are shown in Scheme 1. Variation of the side group was found to modify the surface morphology and wettability without the use of any secondary functionalization. Additionally, it was found that many of these monomers could yield surfaces with  $\theta_{\text{water}} > 150^\circ$ , even though the polymers were determined to be intrinsically hydrophilic.



**Scheme 1** Original monomers synthesized and studied in this work.

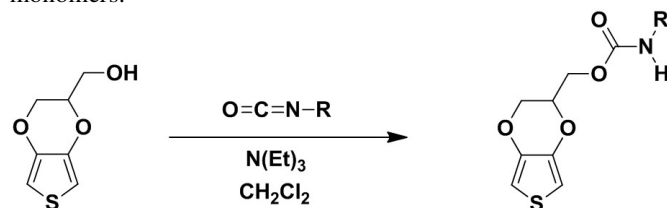
## 2. Experimental

### 2.1. Materials

Hydroxymethyl-EDOT and all isocyanates (ethyl, butyl, hexyl, octyl, decyl, dodecyl, tert-butyl, phenyl, diphenyl methyl, 4-biphenyl, 2-naphthyl) were used as received (Aldrich) and without further purification.

### 2.2. Monomer Synthesis

The monomers were synthesized by reacting an isocyanate with hydroxymethyl-EDOT to form a carbamate linker between EDOT and the side group (Scheme 2). In brief, 1.45 mmol (250 mg) of hydroxymethyl EDOT and 1.74 mmol of the chosen isocyanate were dissolved in 20 mL of anhydrous dichloromethane. Approximately 10 drops (1.5 mL) of triethylamine was added as catalyst. The mixture was stirred at  $40^\circ\text{C}$  for 24 h. The products were purified using column chromatography on silica gel with dichloromethane/methanol 19:1 as eluent for the product with ethyl isocyanate as a reactant, and dichloromethane as eluent for the rest of the monomers.



**Scheme 2** Synthetic route to monomers.

### (2,3-dihydrothieno[3,4-*b*][1,4]dioxin-2-yl)methyl ethylcarbamate (ECOT-C2).

Yield 70%; White solid; m.p.  $68.0^\circ\text{C}$ ;  $\delta_{\text{H}}$ (200 MHz,  $\text{CDCl}_3$ ): 6.36 (1 H, d,  $J$  3.7), 6.33 (1 H, d,  $J$  3.7), 4.77 (1 H, m), 4.32 (4 H, m), 4.01 (1 H, dd,  $J$  11.7,  $J$  7.1), 3.23 (2 H, quint,  $J$  7.2), 1.14 (3 H, t,  $J$  7.2);  $\delta_{\text{C}}$ (200 MHz,  $\text{CDCl}_3$ ): 155.66, 141.26, 141.16, 99.96, 99.83, 71.96, 65.65, 62.67, 36.00, 15.14; FTIR (KBr):  $\nu_{\text{max}}/\text{cm}^{-1}$  3297, 3120, 2974, 2935, 2896, 1692, 1550, 1488, 1260, 1185, 1017, 757  $\text{cm}^{-1}$ ; MS (70 eV):  $m/z$  243 ( $\text{M}^+$ , 10), 154 ( $\text{C}_7\text{H}_6\text{O}_2\text{S}^+$ , 100).

### (2,3-dihydrothieno[3,4-*b*][1,4]dioxin-2-yl)methyl butylcarbamate (EDOT-C4).

Yield 33%; White solid; m.p.  $36.8^\circ\text{C}$ ;  $\delta_{\text{H}}$ (200 MHz,  $\text{CDCl}_3$ ): 6.36 (1 H, d,  $J$  3.7), 6.33 (1 H, d,  $J$  3.7), 4.79 (1 H, m), 4.28 (4 H, m), 4.01 (1 H, dd,  $J$  11.7,  $J$  7.1), 3.18 (2 H, q,  $J$  6.5), 1.39 (4 H, m), 0.92 (3 H, t,  $J$  7.1);  $\delta_{\text{C}}$ (200 MHz,  $\text{CDCl}_3$ ): 155.76, 141.24, 141.14, 99.94, 99.81, 71.97, 65.63, 62.65, 41.16, 31.38, 29.78, 26.34, 22.50, 13.96; FTIR (KBr):  $\nu_{\text{max}}/\text{cm}^{-1}$  3345, 3112, 2961, 2935, 2870, 1688, 1537, 1488, 1245, 1185, 1026, 755  $\text{cm}^{-1}$ ; MS (70 eV):  $m/z$  271 ( $\text{M}^+$ , 14), 154 ( $\text{C}_7\text{H}_6\text{O}_2\text{S}^+$ , 100).

### (2,3-dihydrothieno[3,4-*b*][1,4]dioxin-2-yl)methyl hexylcarbamate (EDOT-C6).

Yield 48%; White solid; m.p.  $47.0^\circ\text{C}$ ;  $\delta_{\text{H}}$ (200 MHz,  $\text{CDCl}_3$ ): 6.36 (1 H, d,  $J$  3.7), 6.33 (1 H, d,  $J$  3.7), 4.81 (1 H, m), 4.30 (4 H, m), 4.01 (1 H, dd,  $J$  11.7,  $J$  7.1), 3.17 (2 H, q,  $J$  6.7), 1.49 (2 H, m), 1.28 (6 H, m), 0.88 (3 H, t,  $J$  6.5);  $\delta_{\text{C}}$ (200 MHz,  $\text{CDCl}_3$ ): 155.76, 141.24, 141.14, 99.94, 99.81, 71.97, 65.63, 62.65, 41.16, 31.38, 29.78, 26.34, 22.50, 13.96; FTIR (KBr):  $\nu_{\text{max}}/\text{cm}^{-1}$  3340, 3125, 2957, 2935, 2853, 1686, 1537, 1492, 1256, 1185, 1017, 753  $\text{cm}^{-1}$ ; MS (70 eV):  $m/z$  299 ( $\text{M}^+$ , 10), 154 ( $\text{C}_7\text{H}_6\text{O}_2\text{S}^+$ , 100).

### (2,3-dihydrothieno[3,4-*b*][1,4]dioxin-2-yl)methyl octylcarbamate (EDOT-C8).

Yield 52%; White solid; m.p.  $55.0^\circ\text{C}$ ;  $\delta_{\text{H}}$ (200 MHz,  $\text{CDCl}_3$ ): 6.36 (1 H, d,  $J$  3.7), 6.33 (1 H, d,  $J$  3.7), 4.79 (1 H, m), 4.28 (4 H, m), 4.01 (1 H, dd,  $J$  11.7,  $J$  7.1), 3.17 (2 H, q,  $J$  6.6), 1.49 (2 H, m), 1.26 (10 H, m), 0.87 (3 H, t,  $J$  6.4);  $\delta_{\text{C}}$ (200 MHz,  $\text{CDCl}_3$ ): 155.76, 141.26, 141.16, 99.95, 99.83, 71.99, 65.65, 62.67, 41.18, 31.74, 29.84, 29.18, 26.69, 22.60, 14.06; FTIR (KBr):  $\nu_{\text{max}}/\text{cm}^{-1}$  3340, 3125, 2961, 2927, 2849, 1686, 1535, 1492, 1245, 1183, 1017, 755  $\text{cm}^{-1}$ ; MS (70 eV):  $m/z$  327 ( $\text{M}^+$ , 8), 154 ( $\text{C}_7\text{H}_6\text{O}_2\text{S}^+$ , 100).

### (2,3-dihydrothieno[3,4-*b*][1,4]dioxin-2-yl)methyl decylcarbamate (EDOT-C10).

Yield 12%; White solid; m.p.  $64.9^\circ\text{C}$ ;  $\delta_{\text{H}}$ (200 MHz,  $\text{CDCl}_3$ ): 6.36 (1 H, d,  $J$  3.7), 6.33 (1 H, d,  $J$  3.7), 4.77 (1 H, m), 4.27 (4 H, m), 4.01 (1 H, dd,  $J$  11.7,  $J$  7.1), 3.17 (2 H, q,  $J$  6.7), 1.49 (2 H, m), 1.26 (14 H, m), 0.88 (3 H, t,  $J$  6.4);  $\delta_{\text{C}}$ (200 MHz,  $\text{CDCl}_3$ ): 155.77, 141.27, 141.14, 99.96, 99.83, 72.00, 65.66, 62.68, 41.19, 31.86, 29.86, 29.51, 29.27, 29.23, 26.70, 22.655, 14.09; FTIR (KBr):  $\nu_{\text{max}}/\text{cm}^{-1}$  3345, 3129, 2956, 2922, 2845, 1688, 1533, 1492, 1256, 1183, 1017, 757  $\text{cm}^{-1}$ ; MS (70 eV):  $m/z$  355 ( $\text{M}^+$ , 4), 215 ( $\text{C}_{17}\text{H}_{11}^{+}$ , 100).

### (2,3-dihydrothieno[3,4-*b*][1,4]dioxin-2-yl)methyl dodecylcarbamate (EDOT-C12).

Yield 37%; White solid; m.p. 68.5°C;  $\delta_{\text{H}}$ (200 MHz,  $\text{CDCl}_3$ ): 6.36 (1 H, d,  $J$  3.7), 6.33 (1 H, d,  $J$  3.7), 4.79 (1 H, m), 4.30 (4 H, m), 4.01 (1 H, dd,  $J$  11.7,  $J$  7.1), 3.17 (2 H, q,  $J$  6.6), 1.48 (2 H, m), 1.25 (18 H, m), 0.87 (3 H, t,  $J$  6.4);  $\delta_{\text{C}}$ (200 MHz,  $\text{CDCl}_3$ ): 155.76, 141.26, 141.16, 99.96, 99.83, 71.99, 65.65, 62.67, 41.18, 31.89, 29.85, 29.60, 29.55, 29.51, 29.32, 29.23, 22.66, 14.10; FTIR (KBr):  $\nu_{\text{max}}/\text{cm}^{-1}$  3345, 3125, 2953, 2922, 2845, 1689, 1534, 1491, 1245, 1185, 1017, 753  $\text{cm}^{-1}$ .

**(2,3-dihydrothieno[3,4-*b*][1,4]dioxin-2-yl)methyl tert-butylcarbamate (EDOT-tBu).**

Yield 34%; White solid; m.p. 95.4°C;  $\delta_{\text{H}}$ (200 MHz,  $\text{CDCl}_3$ ): 6.36 (1 H, d,  $J$  3.7), 6.33 (1 H, d,  $J$  3.7), 4.76 (1 H, m), 4.26 (4 H, m), 4.01 (1 H, dd,  $J$  11.7,  $J$  7.4), 1.32 (9 H, s);  $\delta_{\text{C}}$ (200 MHz,  $\text{CDCl}_3$ ): 154.00, 141.26, 141.19, 99.92, 99.78, 72.06, 65.69, 62.10, 50.53, 28.80; FTIR (KBr):  $\nu_{\text{max}}/\text{cm}^{-1}$  3336, 3112, 2974, 2913, 2870, 1705, 1537, 1484, 1275, 1185, 1026, 755  $\text{cm}^{-1}$ ; MS (70 eV):  $m/z$  271 ( $\text{M}^+$ , 15), 154 ( $\text{C}_7\text{H}_6\text{O}_2\text{S}^+$ , 100).

**(2,3-dihydrothieno[3,4-*b*][1,4]dioxin-2-yl)methyl phenylcarbamate (EDOT-Ph).**

Yield 97%; Colourless liquid;  $\delta_{\text{H}}$ (200 MHz,  $\text{CDCl}_3$ ): 7.35 (4 H, m), 7.09 (1 H, m), 6.73 (1 H, m), 6.39 (1 H, d,  $J$  3.7), 6.36 (1 H, d,  $J$  3.7), 4.42 (3 H, m), 4.27 (1 H, dd,  $J$  11.7,  $J$  1.9), 4.07 (1 H, dd,  $J$  11.7,  $J$  6.8);  $\delta_{\text{C}}$ (200 MHz,  $\text{CDCl}_3$ ): 152.76, 141.17, 140.98, 137.32, 129.13, 123.86, 118.77, 100.11, 100.02, 71.76, 65.54, 63.06; FTIR (KBr):  $\nu_{\text{max}}/\text{cm}^{-1}$  3366, 3107, 2948, 29226, 2870, 1716, 1533, 1488, 1226, 1198, 1058, 760  $\text{cm}^{-1}$ .

**(2,3-dihydrothieno[3,4-*b*][1,4]dioxin-2-yl)methyl benzhydrylcarbamate (EDOT-DiPh).**

Yield 78%; White solid; m.p. 107.4°C; 7.28 (10 H, m), 6.73 (1 H, m), 6.34 (1 H, d,  $J$  3.3), 6.32 (1 H, d,  $J$  3.3), 5.96 (1 H, d,  $J$  7.6), 5.49 (1 H, d,  $J$  7.6), 6.32 (1 H, d,  $J$  3.7), 4.28 (4 H, m), 4.00 (1 H, dd,  $J$  11.4,  $J$  6.2);  $\delta_{\text{C}}$ (200 MHz,  $\text{CDCl}_3$ ): 154.98, 141.29, 141.20, 141.08, 128.72, 127.62, 127.17, 99.97, 99.86, 71.86, 65.55, 63.03, 58.98; FTIR (KBr):  $\nu_{\text{max}}/\text{cm}^{-1}$  3296, 3115, 2957, 2912, 2868, 1688, 1535, 1488, 1236, 1185, 1024, 700  $\text{cm}^{-1}$ .

**(2,3-dihydrothieno[3,4-*b*][1,4]dioxin-2-yl)methyl [1,1'-biphenyl]-4-ylcarbamate (EDOT-BiPh).**

Yield 98%; White solid; m.p. 156.5°C;  $\delta_{\text{H}}$ (200 MHz,  $\text{CDCl}_3$ ): 7.46 (10 H, m), 6.40 (1 H, d,  $J$  3.7), 6.36 (1 H, d,  $J$  3.7), 4.44 (3 H, m), 4.28 (1 H, dd,  $J$  11.7,  $J$  2.0), 4.08 (1 H, dd,  $J$  11.7,  $J$  7.2);  $\delta_{\text{C}}$ (200 MHz,  $\text{CDCl}_3$ ): 152.77, 141.16, 140.97, 140.37, 136.79, 136.61, 128.77, 128.62, 127.98, 127.75, 127.10, 126.79, 126.37, 126.23, 119.08, 100.12, 100.04, 71.75, 65.53, 63.14; FTIR (KBr):  $\nu_{\text{max}}/\text{cm}^{-1}$  3371, 3094, 2957, 2926, 2870, 1716, 1533, 1492, 1221, 1200, 1058, 763  $\text{cm}^{-1}$ .

**(2,3-dihydrothieno[3,4-*b*][1,4]dioxin-2-yl)methyl naphthalen-2-ylcarbamate (EDOT-Na).**

Yield 94%; White solid; m.p. 155.6°C;  $\delta_{\text{H}}$ (200 MHz,  $\text{DCO-N}(\text{CD}_3)_2$ ): 7.71 (7 H, m), 6.67 (1 H, d,  $J$  3.7), 6.64 (1 H, d,  $J$  3.7), 4.49 (4 H, m), 4.16 (1 H, dd,  $J$  11.7,  $J$  7.5);  $\delta_{\text{C}}$ (200 MHz,  $\text{DCO-N}(\text{CD}_3)_2$ ): 153.88, 141.94, 137.43, 134.37, 130.27, 128.92, 127.89, 127.52, 126.78, 124.69, 119.70, 114.31, 100.20, 100.15, 72.47, 65.81, 63.05; FTIR (KBr):  $\nu_{\text{max}}/\text{cm}^{-1}$  3379, 3099, 2952, 2922, 2870, 1727, 1539, 1482, 1221, 1183, 1058, 763  $\text{cm}^{-1}$ .

Infrared spectra of the monomers were obtained using a Spectrum 100 FT-IR spectrometer (Perkin Elmer) with 4  $\text{cm}^{-1}$  resolution in transmission mode. NMR spectra were recorded with a W-200MHz (Bruker). Melting points of monomers were determined via differential scanning calorimetry (Jade DSC-Perkin Elmer), using a thermal scan from -25°C to 150°C at a rate of 10°C/min.

## 2.3. Electropolymerization

The polymer films were formed using a Metrohm potentiostat (Autolab). For all experiments a 2  $\text{cm}^2$  gold plate was used as the working electrode, a carbon-rod was used as the counter electrode, and a saturated calomel electrode (SCE) was used as the reference. A 0.1 M solution of tetrabutylammonium ( $\text{Bu}_4\text{NClO}_4$ ) in anhydrous acetonitrile was used as electrolyte and 10 mmol of each monomer was added prior to electropolymerization. Cyclic voltammetry was used to obtain the films using 20  $\text{mV s}^{-1}$  as the scan rate and the scans were done between -1.0 V to a value slightly lower than the monomer oxidation potential. This method was chosen as it allows for the deposition of highly homogeneous and adherent films. Films were prepared with 1, 3, and 5 deposition scans to study polymer growth on the surfaces. Examples of cyclic voltammograms are given in Figure 1. Extremely well defined cyclic voltammograms with multiple oxidation and reduction peaks characteristic of PEDOT polymers are obtained. For example, the influence of the alkyl chain length is not significant. Hence, quite the same polymer chain lengths are obtained whatever the alkyl chain length, which is due to the exceptional polymerization capacity of EDOT. Using aromatic cycles the substituent effect is more significant and the polymer chain lengths are reduced. Moreover, when using EDOT-Na the presence of naphthalene groups causes extreme steric hindrance, leading to short polymer chain lengths (Figure 1). Analogous “smooth” surfaces of each polymer were formed via electropolymerization to obtain the Young’s angle ( $\theta^{\text{Y}}$ ). The smooth films were formed with an imposed potential ( $\sim 1.2$  V vs SCE) and a low deposition charge (1  $\text{mC cm}^{-2}$ ).

## 2.4. Surface Characterization

Contact angle measurements were done using a DSA30 goniometer (Krüss). Apparent contact angles ( $\theta$ ) were measured using the sessile method with 2  $\mu\text{L}$  droplets of liquids of varying surface tensions ( $\gamma_{\text{LV}}$ ): water (72.8  $\text{mN/m}$ ), diiodomethane (50.0  $\text{mN/m}$ ) and hexadecane (27.6  $\text{mN/m}$ ). When the surfaces had strong anti-wetting properties (contact angles greater than 150°) 10  $\mu\text{L}$  droplets were used since the deposition of 2  $\mu\text{L}$  droplets was very difficult. Water adhesion on the surfaces was measured using dynamic contact angles. A 10  $\mu\text{L}$  droplet was placed on the polymer and the surface was inclined until the droplet “rolled-off” (tilted-drop method). The contact angles in the front and the back of the droplet just before rolling off ( $\theta_{\text{adv}}$  and  $\theta_{\text{rec}}$ ) were measured to determine the hysteresis:  $H = \theta_{\text{adv}} - \theta_{\text{rec}}$ . If the water droplet never rolled off the surface, up to an

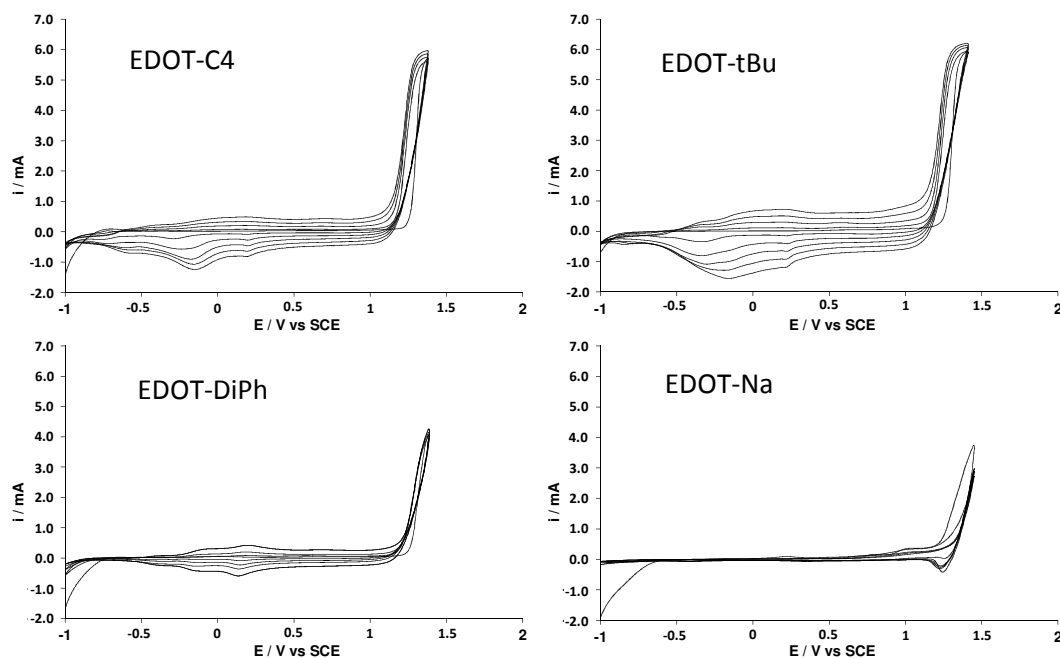


Fig. 1 Cyclic voltammogram of different monomers (5 scans) recorded in  $\text{Bu}_4\text{NClO}_4/\text{anhydrous acetonitrile}$  and at a scan rate of  $20 \text{ mV s}^{-1}$ .

inclination of  $90^\circ$  it was classified as “sticky”. The maximum inclination angle of the surface prior to roll-off was taken as the sliding angle ( $\alpha$ ). Mean arithmetic ( $R_a$ ), mean quadratic ( $R_q$ ) roughness, and roughness factor ( $r$ ) of the surfaces were determined with optical profilometry (Wyko NT 1100, Bruker). The measurements were done using High Mag Phase Shift Interference (PSI), 50X objective and 0.5X field of view. Surface morphology was characterized with scanning electron microscopy (SEM, 6700F microscope, JEOL).

### 3. Results and Discussion

#### 3.1 Morphology / Roughness

Two control parameters are available to tune surface morphology with electrodeposition: electrochemical factors and monomer structure. In this study the conditions of the electropolymerization are held constant, so only the monomer structure can influence the resulting surface morphology. The surface morphologies of selected alkyl- and aromatic-substituted EDOT monomers by SEM after 3 deposition scans are given in Figures 2 and 3. The roughness data of all polymer films after 1, 3, and 5 deposition scans is summarized in Table 1, including the roughness factor  $r$  used in the Cassie-Baxter and Wenzel equations of wetting, which will be discussed in detail with the wettability studies. As expected, the surface roughness increases with the number of deposition scans for each monomer. Typically highly structured surfaces result if the solubility of the oligomer formed in solution is very low, and if the oligomer solubility is very high smoother surfaces will form. Here, with the electrochemical parameters being constant, the most common factors affecting oligomer solubility are substituent hydrophobicity and the polymer chain length.

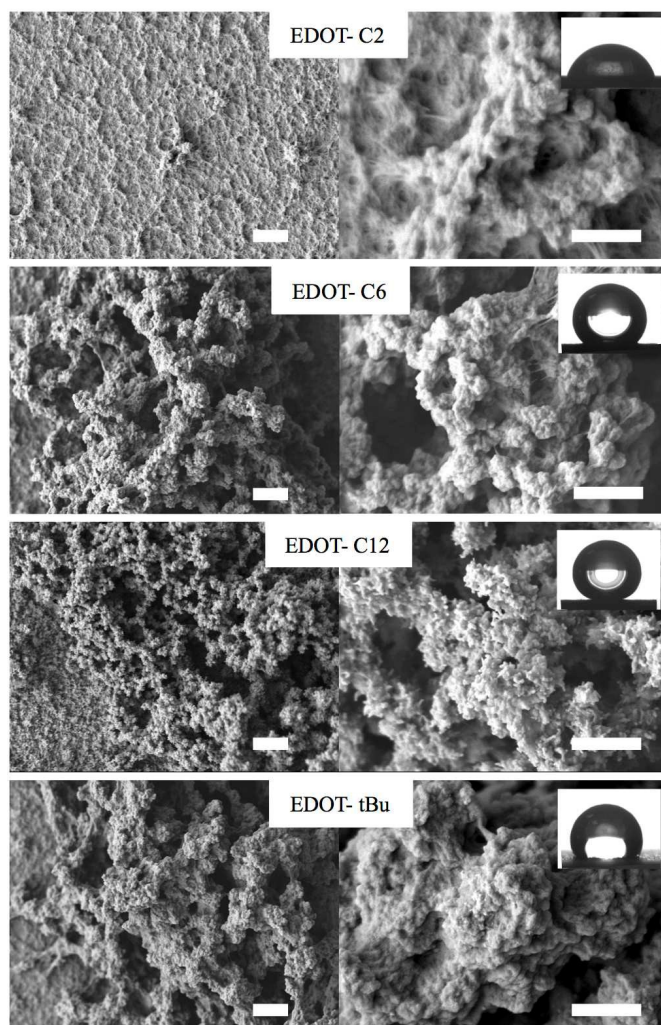


**Fig. 2** SEM Images at two magnifications (5,000X and 25,000X) for EDOT-C2, EDOT-C6, EDOT-C12 and EDOT-tBu after 3 deposition scans. Scale bar indicates 2.5  $\mu\text{m}$  for images at 5,000X magnification (left) and 1  $\mu\text{m}$  for images at 25,000X magnification (right). Optical images of water contact angles with each surface are included (inset).

A clear trend of increasing roughness with increasing alkyl chain length is observed (Figure 2). The deposition of EDOT-C2 forms a relatively smooth surface with nano-scale topography ( $R_a \sim 580\text{nm}$ ) that increases to micron scale roughness with alkyl chains greater than  $C_8$  (Table 1). This is not surprising, as increases in alkyl chain length are expected to decrease oligomer solubility in solution, forming rougher films. When the side group is *tert*-butyl (EDOT-tBu) the surface is marginally rougher than the EDOT-C4 substrate, indicating that there are slight differences in solubility based on the branching of the alkyl chain.

When the side group substituent is alkyl in nature, the surface morphology consists of large agglomerates. As the alkyl length increases, there is dual-scale nano-fiber structure present on the deposited polymer, as observed in the EDOT-C12 SEM image (Figure 2). Once the alkyl chain length is  $C_8$  or greater, the oligomer solubility does not change significantly with increases in side group chain length. This is why the deposition of EDOT-C8 forms the roughest surfaces (Table 1) compared to longer alkyl side groups EDOT-C10 and EDOT-C12

**Table 1** Surface roughness as a function of polymer and number of deposition scans.

Polymer	Number of deposition scans	$R_a$ [nm]	$R_q$ [nm]	$r$
EDOT-C2	1	10	12	1.0
	3	580	2200	3.3
	5	820	5750	15
EDOT-C4	1	9	15	1.0
	3	250	1500	1.2
	5	1350	7390	16
EDOT-C6	1	12	19	1.0
	3	490	2110	3.3
	5	1930	5930	34
EDOT-C8	1	37	47	1.0
	3	2940	7640	11
	5	9140	26900	175
EDOT-C10	1	19	27	1.0
	3	1600	5590	3.7
	5	6090	20900	80
EDOT-C12	1	20	26	1.0
	3	1230	4870	5.9
	5	4580	9810	45
EDOT-tBu	1	27	38	1.0
	3	836	2720	9.6
	5	1340	4570	24
EDOT-Ph	1	10	20	1.0
	3	180	790	1.0
	5	1170	4680	26
EDOT-	1	110	140	1.1

DiPh	3	230	330	2.1
	5	560	1190	9.0
EDOT-BiPh	1	14	18	1.0
	3	43	100	1.0
	5	84	170	1.1
EDOT-Na	1	5	7	1.0
	3	17	40	1.0
	5	51	170	1.0

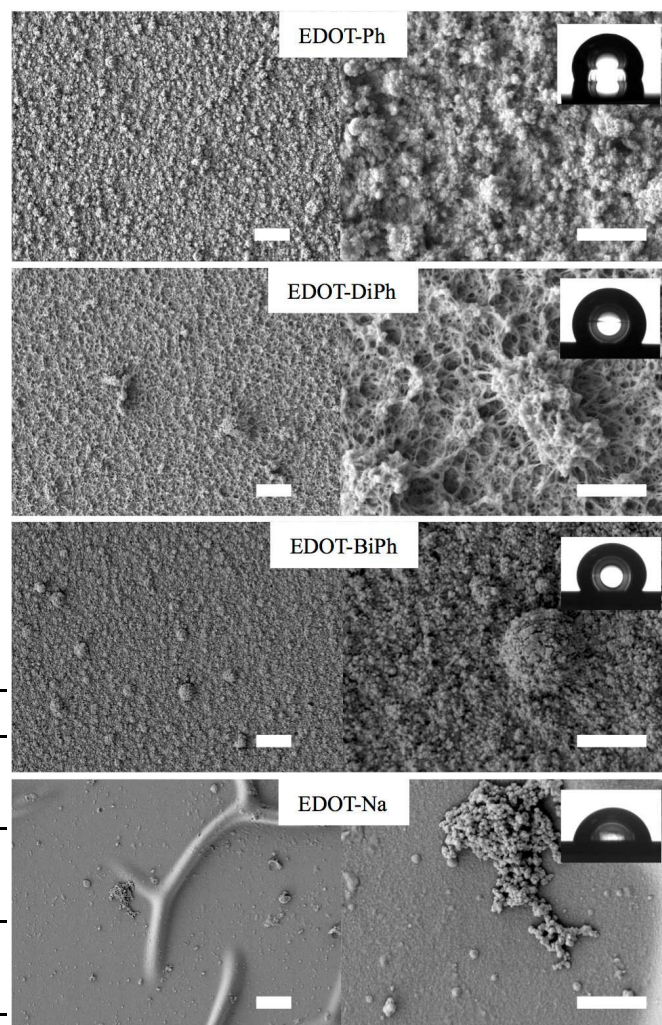


**Fig. 3** SEM Images at two magnifications (5,000X and 25,000X) for EDOT-Ph, EDOT-DiPh, EDOT-BiPh and EDOT-Na after 3 deposition scans. Scale bar indicates 2.5  $\mu\text{m}$  for images at 5,000X magnification (left) and 1  $\mu\text{m}$  for images at 25,000X magnification (right). Optical images of water contact angles with each surface are included (inset).

**Table 2** Apparent contact angles with water ( $\theta_{water}$ ), diiodomethane ( $\theta_{diiodo}$ ) and hexadecane ( $\theta_{hexadecane}$ ) as well as hysteresis (H) behavior and tilting angles ( $\alpha$ ) as a function of the polymer and number of deposition scans.

Polymer	Number of deposition scans	$\theta_{water}$	H <sub>water</sub>	$\alpha_{water}$	$\theta_{diiodo}$	$\theta_{hexadecane}$
EDOT-C2	1	66.8	-	sticky	44.9	0.9
	3	76.5	-	sticky	48.6	0
	5	77.4	-	sticky	38.8	0
EDOT-C4	1	87.7	-	sticky	53.6	0
	3	103.1	-	sticky	57.1	0
	5	117.1	-	sticky	77.3	0
EDOT-C6	1	109.9	-	sticky	59.1	0
	3	135.2	-	sticky	75.4	0
	5	155.3	7.4	6.8	117.7	0
EDOT-C8	1	129.8	-	sticky	75.7	0
	3	156.9	2.5	1.6	106.9	0
	5	152.8	3.3	1.7	128.2	0
EDOT-C10	1	135.6	-	sticky	49.3	0
	3	149.9	3.9	3.3	30.3	0
	5	150.3	1.2	1.7	0	0
EDOT-C12	1	138.2	-	sticky	60.8	0
	3	158.1	2.1	1.7	74.2	0
	5	153.1	4.7	2.8	52.3	0
EDOT-tBu	1	88.1	-	sticky	61.6	0
	3	114.4	-	sticky	74.7	0
	5	144.7	-	sticky	94.9	0
EDOT-Ph	1	90.5	-	sticky	43.1	2.9
	3	106.6	-	sticky	9	0
	5	118.1	-	sticky	2.2	0
EDOT-DiPh	1	113.5	-	sticky	15.9	1.3
	3	122.0	-	sticky	5.5	0
	5	129.9	-	sticky	0	0
EDOT-BiPh	1	118.1	-	sticky	31.8	0.9
	3	109.7	-	sticky	18.8	1
	5	103.5	-	sticky	14.4	2.4
EDOT-Na	1	78.5	-	sticky	27.4	8.3
	3	79.0	-	sticky	31.3	1.9
	5	85.8	-	sticky	21.3	0

The morphology varies significantly when the side-group on the EDOT monomer is aromatic-based (Figure 3). Overall, the surface roughness is significantly reduced (Table 1). This is expected, based on the cyclic voltammograms already presented (Figure 1). The aromatic-substituted monomers form much shorter oligomers in solution, and this effect is most significant during the polymerization of EDOT-Na. The reduced chain length of polymers formed in solution result in much smoother, thinner surface films.

The overall surface morphology also varies amongst aromatic substituent. With EDOT-Ph, EDOT-BiPh and EDOT-Na there is again observed agglomerate morphology. The number of agglomerates and overall surface roughness decreases significantly from EDOT-Ph to EDOT-BiPh, and even more dramatically so on EDOT-Na surfaces that have very few clusters of spherical agglomerates across the entire surface. On the EDOT-Na surface, there are also large wrinkles observed. These are not evidence of secondary surface structuration. Overall, the wrinkles are very small and do not contribute significantly to the overall surface roughness of EDOT-Na surfaces, which are the smoothest surfaces formed in this study (Table 1). Lastly, the EDOT-DiPh monomer forms a more fibrous morphology than the other aromatic substituents.

### 3.2. Wettability

A summary of the mean contact angles with water, diiodomethane and hexadecane, as well as the adhesive behavior observed with water is given in Table 2. With three deposition scans,  $\theta_{water} > 150^\circ$  is observed for EDOT-C8, EDOT-C10 and EDOT-C12, which can be explained by the presence of micro and nano structure observed on these surfaces (Figure 2, Table 1). Additionally, all of these surfaces have very low water adhesion as indicated by the low hysteresis ( $H_{water} < 5^\circ$ ) and low sliding angles ( $\alpha < 4^\circ$ ) for all cases, rendering them superhydrophobic. As expected, these films also are the most oleophobic and have the highest contact angle with diiodomethane ( $\theta_{diiodo}$ ) due to the surface structure. This behavior is expected, and has been seen previously on surfaces modified with alkyl chains of varying length, however no work has presented a method in which these surfaces can be prepared as rapidly and efficiently as here.<sup>28</sup> The surfaces composed of polymers with shorter alkyl side groups (C2-C6) are much smoother, and therefore are also less hydrophobic. It should be noted that with the highest number of deposition scans tested, 5, EDOT-C6 also displays strong water repellency with  $\theta_{water} > 150^\circ$  and slightly higher water adhesion ( $H_{water} \sim 7.4^\circ$ ,  $\alpha \sim 6.8^\circ$ ) than the EDOT-C8, -C10, and -C12 analogues. The monomers modified with aromatic side groups (EDOT-Ph, EDOT-DiPh, EDOT-BiPh, EDOT-Na) are also less hydrophobic than those substituted with long alkyl chains. This is expected, as these surfaces are less structured, smoother, and thinner than those with alkyl-substituents.

For better comprehension of these results, the contact angles ( $\theta_{water}$ ,  $\theta_{diiodo}$ ,  $\theta_{hexadecane}$ ) were also measured for analogous

“smooth” surfaces, giving the Young angle ( $\theta^Y$ - Table 3).<sup>29</sup> From these results, it can be seen that all polymers, with the exception of EDOT-C12 are intrinsically hydrophilic ( $\theta^Y_{water} < 90^\circ$ ), which can be explained by the high polarity of the carbamate linker. EDOT-C12 is also the most oleophobic, having the highest  $\theta^Y_{diiodo}$  and  $\theta^Y_{hexadecane}$ . It should be noted that for all smooth polymers tested here, the Young angle with hexadecane is negligible ( $\theta^Y_{hexadecane} < 15^\circ$ ). As expected, the monomers with aromatic side groups (EDOT-Ph, EDOT-DiPh, EDOT-BiPh, EDOT-Na) are the most oleophilic, having the lowest contact angles with diiodomethane ( $\theta^Y_{diiodo} < 40^\circ$ ).

**Table 3** Apparent contact angles of “smooth” polymers with water ( $\theta^Y_{water}$ ), diiodomethane ( $\theta^Y_{diiodo}$ ) and hexadecane ( $\theta^Y_{hexadecane}$ ).

Polymer	$\theta^Y_{water}$	$\theta^Y_{diiodo}$	$\theta^Y_{hexadecane}$
EDOT-C2	66.9	47.9	12.5
EDOT-C4	82.2	52.0	10.8
EDOT-C6	86.2	53.2	11.2
EDOT-C8	88.5	56.8	11.4
EDOT-C10	85.7	53.5	8.6
EDOT-C12	94.6	57.8	12.6
EDOT-tBu	85.3	51.7	10.8
EDOT-Ph	80.6	33.9	10.4
EDOT-DiPh	71.4	35.9	11.8
EDOT-BiPh	79.3	21.3	6.4
EDOT-Na	73.8	26.9	11.5

Using both the smooth contact angles ( $\theta^Y$ ) and those observed on rough, micro-structured surfaces the wettability results can be explained in more detail. Two equations are used to explain the wetting of rough surfaces: the Wenzel equation<sup>15</sup> and the Cassie-Baxter equation.<sup>14</sup> The Wenzel equation describes the contact angle ( $\theta$ ) as a function of roughness as follows:

$$\cos \theta = r \cos \theta^Y$$

Here, the roughness parameter  $r$  is the ratio of the actual solid surface area to the geometric surface area. The Wenzel relationship is valid for a surface where a liquid droplet penetrates into all the surface roughness. Following this relationship,  $\theta$  can only be  $> \theta^Y$  when  $\theta^Y > 90^\circ$ . The roughness parameter  $r$ , presented in Table 1, corresponds to this ratio.

In the Cassie-Baxter state, the contact angle is described as:

$$\cos \theta = r_f \cos \theta^Y + f - 1$$

Here  $r_f$  is the roughness ratio of the surface which is wetted, and is defined in the same manner as in the Wenzel equation, and  $f$  is the fraction of the solid surface area that is wetted by the liquid, as described by Marmur in the literature.<sup>30</sup> In this state, the presence of air inside the surface roughness permits the increase of the contact angle, no matter what the value of  $\theta$ .

Since all of the polymers in this work, with the exception of EDOT-C12, have  $\theta_{water}^Y < 90^\circ$ , the Wenzel state does not appropriately describe these surfaces and their interaction with water. Therefore the Cassie-Baxter state, where strong hydrophobicity induced by surface roughness despite intrinsic hydrophilicity of the polymers is possible, describes these substrates. As the roughness increases (either with increased number of deposition scans or increased length of alkyl side group), the increase in air trapped between the water droplets leads to a higher contact angle.

Characterizing the interaction between the polymer surfaces and liquids with lower surface tensions, specifically diiodomethane ( $\gamma_{LV} = 50.0$  mN/m) is more complicated and varies based on side-group. All polymers are intrinsically oleophilic as  $\theta_{diiodo}^Y < 90^\circ$ . Alkyl substituted monomers EDOT-C4, EDOT-C6 and EDOT-C8 follow the Cassie-Baxter state, as increases in surface roughness with number of deposition scans correspond to a larger  $\theta_{diiodo}$ , despite being intrinsically oleophilic. All of the aromatic substituted polymers have a general decrease in  $\theta_{diiodo}$  with increasing number of deposition scans and surface roughness, indicating these surfaces follow the Wenzel state of wetting with diiodomethane. The intrinsic oleophilicity ( $\theta_{diiodo}^Y < 40^\circ$ ) of the aromatic-substituted EDOT monomers permits the complete penetration of diiodomethane into the surface roughness. This rationale can also be used to describe the wetting of diiodomethane onto EDOT-C2 surfaces, which has the lowest  $\theta_{diiodo}^Y$  of all alkyl substituted polymers tested here, and also follows the Wenzel state.

Both EDOT-C10 and EDOT-C12 follow the Wenzel state of wetting with diiodomethane as well, as there is a general decrease in  $\theta_{diiodo}$  with number of deposition scans. The increase from the C8 side group to C10 is critical in this study, as it represents the border at which either the Cassie-Baxter or Wenzel state dominates the wetting of a liquid with lower surface tension, such as diiodomethane. It is likely that as the surface tension decreases further, this border would shift to EDOT polymers with shorter alkyl substituents. This is already apparent in the observed contact angles with hexadecane ( $\theta_{hexadecane}$ ), a liquid with a much lower surface tension ( $\gamma_{LV} = 27.8$  mN/m), where all surfaces are wetted completely.

#### 4. Conclusions

This work reports a facile route to develop micro and nano-structured surfaces using electrodeposition of monomers based on 3,4-ethylenedioxythiophene (EDOT). Both alkyl and aromatic side groups were incorporated onto the EDOT monomer by reacting various isocyanates with a commercially available EDOT derivative (hydroxymethyl-EDOT), forming a carbamate linker between EDOT and the desired side group. The surface roughness and wettability could be tuned based on the side-group incorporated. In general, with increasing alkyl chain length of the side group, rougher more hydrophobic surfaces were formed via electrodeposition. When the alkyl chain length exceeded C8,  $\theta_{water} > 150^\circ$  despite most polymers being intrinsically hydrophilic ( $\theta_{water}^Y < 90^\circ$ ), which follows the

Cassie-Baxter equation of wetting. The aromatic substituted EDOT monomers also followed the same trends of surface wettability with water. The oleophobicity of the surfaces was tested using diiodomethane. All the polymers formed were intrinsically oleophilic ( $\theta_{diiodo}^Y < 90^\circ$ ), but the wetting state with diiodomethane varied based on the side-group incorporated. As the chain length of the alkyl side group increased, the wetting state transitioned from Cassie-Baxter to Wenzel, and all substrates with aromatic-substituted EDOT followed the Wenzel state of wetting. This study shows that by simply adjusting the side group structure, different micro- and nano-structured coatings with varying degrees of wettability can be fabricated. Both the synthesis of the monomers and the electrodeposition procedure are very straightforward and easily replicated, making these substrates attractive for a multitude of applications where hydrophobic surfaces are desired.

#### Acknowledgements

We thank J.P. Laugier and S. Pagnotta from the CCMA (Centre Commun de Microscopie Appliquée) of the Université de Nice Sophia Antipolis for the SEM imaging.

#### Notes and references

<sup>a</sup> Univ. Nice Sophia Antipolis, LPMC, UMR 7336, CNRS, Parc Valrose, 06100 Nice, France

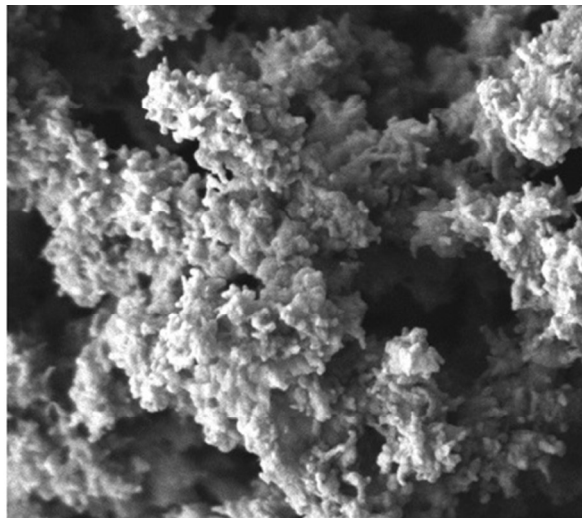
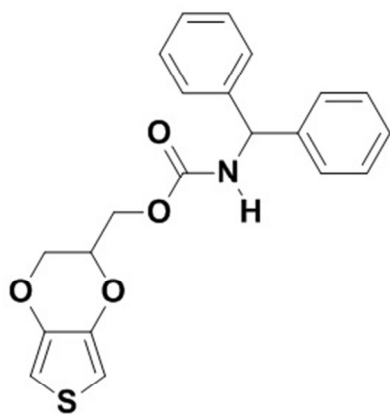
Fax: (+33)4-92-07-61-56; Tel: (+33)4-92-07-61-59;

E-mail: Frederic.GUITTARD@unice.fr

- 1 M. He, J. Wang, H. Li and Y. Song, *Soft Matter*, 2011, **7**, 3993–4000.
- 2 L. Cao, A. K. Jones, V. K. Sikka, J. Wu and D. Gao, *Langmuir*, 2009, **25**, 12444–12448.
- 3 H. A. Stone, *ACS Nano*, 2012, **6**, 6536–6540.
- 4 Y. Lai, Y. Tang, J. Gong, D. Gong, L. Chi, C. Lin and Z. Chen, *J. Mater. Chem.*, 2012, **22**, 7420–7426.
- 5 K.-C. Park, H. J. Choi, C.-H. Chang, R. E. Cohen, G. H. McKinley and G. Barbastathis, *ACS Nano*, 2012, **6**, 3789–3799.
- 6 J. Ballester-Beltrán, P. Rico, D. Moratal, W. Song, J. F. Mano and M. Salmerón-Sánchez, *Soft Matter*, 2011, **7**, 10803–10811.
- 7 M. Zhang, C. Wang, S. Wang, Y. Shi and J. Li, *Appl. Surf. Sci.*, 2012, **261**, 764–769.
- 8 W. Zhang, Z. Shi, F. Zhang, X. Liu, J. Jin and L. Jiang, *Adv. Mater.*, 2013, **25**, 2071–2076.
- 9 T. Darmanin and F. Guittard, *Materials Today*, 2015, **18**, 273–285.
- 10 M. Nosonovsky and B. Bhushan, *Adv. Funct. Mater.*, 2008, **18**, 843–855.
- 11 B. Bhushan and Y. C. Jung, *J. Phys.: Condens. Matter*, 2008, **20**, 225010.
- 12 X.-M. Li, D. Reinhoudt and M. Crego-Calama, *Chem. Soc. Rev.*, 2007, **36**, 1350–1368.
- 13 P. Roach, N. J. Shirtcliffe and M. I. Newton, *Soft Matter*, 2008, **4**, 224–240.
- 14 A. Cassie and S. Baxter, *Trans. Faraday Soc.*, 1944.
- 15 R. N. Wenzel, *Ind. Eng. Chem.*, 1936, **28**, 988–994.
- 16 A. Marmur, *Soft Matter*, 2012, **8**, 6867–6870.
- 17 K. Liu, J. Du, J. Wu and L. Jiang, *Nanoscale*, 2012, **4**, 768–772.
- 18 Lin Feng, Yanan Zhang, Jinming Xi, Ying Zhu, Nü Wang, A. Fan XiaLei Jiang, *Langmuir*, 2008, **24**, 4114–4119.
- 19 J. B. K. Law, A. M. H. Ng, A. Y. He and H. Y. Low, *Langmuir*, 2014, **30**, 325–331.
- 20 X. Lu, H. Cai, Y. Wu, C. Teng, C. Jiang, Y. Zhu and L. Jiang, *Sci. Bull.*, 2015, **60**, 453–459.
- 21 M. Jin, X. Feng, L. Feng, T. Sun, J. Zhai, T. Li and L. Jiang, *Adv. Mater.*, 2005, **17**, 1977–1981.
- 22 H. Bellanger, T. Darmanin, E. T. de Givenchy and F. Guittard, *Chem. Rev.*, 2014, **114**, 2694–2716.

## Journal Name

- 23 J. El Maiss, T. Darmanin and F. Guittard, *RSC Adv.*, 2015, **5**, 37196–37205.
- 24 T. Darmanin and F. Guittard, *Synth. Met.*, 2015, **205**, 58–63.
- 25 G. Godeau, J. N'Na, T. Darmanin and F. Guittard, *J. Phys. Chem. B*, 2015, **119**, 6873–6877.
- 26 M. Wolfs, T. Darmanin and F. Guittard, *Surf. Coat. Technol.*, 2014, **259**, 594–598.
- 27 T. Darmanin and F. Guittard, *Adv. Mater. Interfaces*, 2015, **2**, 1500081–1500087.
- 28 S. Wang, L. Feng, H. Liu, T. Sun, X. Zhang, L. Jiang and D. Zhu, *ChemPhysChem*, 2005, **6**, 1475–1478.
- 29 T. Y. Young, *Philos. Trans. R. Soc. London*, 1805, 1–24.
- 30 A. Marmur, *Langmuir*, 2008, **24**, 7573–7579.



182x93mm (96 x 96 DPI)